



KINETIC AND ISOTHERM EVALUATION OF *O*-CRESOL ADSORPTION ON ACTIVATED CARBON PROCURED FROM OLIVE POMACE

*Salima CHOUKCHOU BRAHAM, Zoubida TALEB, Soumia DJEZIRI, Hadja Mebarka DJELLOULI**

Laboratory of Materials & Catalysis, Faculty of Exact Sciences, Djillali Liabes University, BP 89, Sidi Bel Abbes, Algeria

Received: 18 March 2023

Revised: 02 May 2023

Accepted: 04 May 2023

This article aims to apply an activated carbon on the adsorption of o-cresol in an aqueous medium. Our work presents a double environmental aspect: On one hand, a valorization of under-natural products, which is the olive pomace and on the other hand, the study of the adsorbent efficiency of the activated carbon resulting from these cores. Activated carbon is prepared with chemical activation of olive pomace using H_3PO_4 . The characterization of this porous material has shown a specific surface area equal to $651 \text{ m}^2/\text{g}$ with the presence of mesopores. Various parameters influencing the adsorption were optimized, mainly the effect of the contact time, initial concentration of o-cresol and pH of the solution were studied. The experimental results show that the sorption equilibrium is reached within 60 min with an adsorption yields of 83.66%. Indeed, the experimental adsorbed quantity of adsorbent is 3.82 mg/g with o-cresol concentration of 50 mg/L, $T = 30 \text{ }^\circ\text{C}$ and pH 2.6 for the better adsorption.

The adsorption process was also studied by examining Langmuir, Freundlich, Temkin isotherm, and Dubinin–Radushkevich (D-R) isotherm models. The results revealed that the adsorption system followed the pseudo-second order model and the Freundlich model. Several thermodynamic factors, namely, the standard free energy (ΔG_{ads}), enthalpy (ΔH_{ads}), and entropy (ΔS_{ads}) changes, were also calculated. The results demonstrated that the adsorption process is a physical and endothermic. The obtained results are interesting, and applications on other pollutants, in wastewater are in progress.

Keywords: *o*-Cresol, Olive Pomace, Removal, Activated carbon, Isotherm.

INTRODUCTION

The adsorption process with low cost natural minerals is an attractive option because of their efficient removal rate for organic pollutants at even trace levels. Well-designed adsorption processes provide high-quality effluent after treatment. In recent years, considerable attention has been focused on the utilization of pomace such as from deoiled red raspberry pomace (1), cranberry pomace (2) and apple pomace (3-6). Also, the grape pomace mainly composed of seeds, skins and stalks, all containing high amounts of valuable phytochemicals, is the main solid residue of wine industry and is also used (7). In the other hand, olive production is one of the important human activities through the transformation of olive into olive oil and olive table. The olive oil production in Mediterranean countries is more than 94% of world olive oil production (8, 9). Olive dry cake olive pomace also

* Corresponding author: Hadja Mebarka DJELLOULI, Laboratory of Materials & Catalysis, Djillali Liabes University, Faculty of Exact Sciences, Djillali Liabes University, BP 89, Sidi Bel Abbs, Algeria.
e-mail: mebarkad@yahoo.fr



referred to as olive pomace is generated from the extraction of olive oil. Olive pomace contains, in addition to its content, fruit components such as crushed olive stone pieces, olive pulp with residual oil, and 65% water from olive oil extraction (10, 11). Nieto et al. (12) studied the adsorption of Fe by olive stones in agricultural wastewaters. The percentage of iron adsorption increased from 30 to 70% when the initial biomass concentration rose from 25 to 125 g dm⁻³. Bohli et al. (13) examined adsorption of phenol on a prepared activated carbon activated chemically (by H₃PO₄). Authors tested effect of pH, initial concentration (C₀: 25-300 mg/L) and equilibrium time. The results show that activated carbon from olive stone can be used for adsorption of phenol from aqueous solution.

Cresol compounds are substituted phenols which are generated by petroleum and petrochemical, coal conversion, cresols producing industries, and other chemical processes, are common contaminants in wastewater. Cresols are widely used for the commercial production of a wide variety of resins including phenolic resins, which are used as construction materials for epoxy resins and adhesives. Cresols as a class of organics that are resistant to biodegradation. Cresols are previously eliminated from wastewaters using different methods such as adsorption, chemical precipitation, ozonation, ion exchange, filtration, membrane separation, and reverse osmosis (14, 15). Gracioso et al. studied removal of phenolic *o*-cresol from raw industrial wastewater containing a mixture of phenols, *m*-cresol, *o*-cresol, 90% biodegradation was achieved after 80 h of inoculation (16).

The aims of this work were as follows: first, to study the *o*-cresol adsorption kinetics on activated carbon from olive pomace; second, to assess the initial *o*-cresol concentration and adsorbent amount effect on matter transfer rate. Eventually, to find a simple mathematical model suitable for a better understanding of the physical phenomena involved in a more appropriate design, operation, optimization, and control of the industrial process separation. Simplified isotherm models are tested to describe the adsorption process. Kinetics are determined using different models and then correlated with the experimental variables.

EXPERIMENTAL

ACTIVATED CARBON

Activated carbon (AC) was prepared from olive pomace by chemical activation with orthophosphoric acid (H₃PO₄) according to the method developed by Gharib and *al.* (17): Initially, the precursor was washed thoroughly with hot water, dried and then impregnated with a dilute phosphoric acid solution for 6 hours at 110 °C. The resulting material was washed with distilled water to remove all leachable impurities. The dried solid was carbonized in a muffle furnace (NaberTherm B180). The optimized carbonization time and temperature were 1 h and 600 °C, respectively. The producer of carbon was washed with distilled water and then dried to be ready for use.

Specific surface area of prepared activated carbon was determined by nitrogen adsorption and desorption isotherms at 77.7 K with an automatic Sorptiometer Autosorbe-1C Quantachrome apparatus. The specific surface area and pore volumes were calculated by applying Brunauer-Emmett-Teller (BET) analysis method. The point of zero charge (pH_{PZC}), pH at which the adsorbent is neutral in aqueous suspension, was determined following the procedure of Altener (18) et al. In this method, 50 mL of 0.01M NaCl solution was filled in closed



Erlenmeyer flasks at room temperature. Then, the pH of the solutions was modified to values from 2 and 12 by adding 0.1M HCl or 0.1M NaOH solutions. These pHs were mentioned as the initial pH ($pH_{initial}$). Finally, 0.1g of solid adsorbent (AC) was added to each flask and the final pH (pH_{final}) was measured after 24 h. The pH_{final} was plotted against the $pH_{initial}$ and the pH_{PZC} is the point where the curve pH_{final} versus $pH_{initial}$ intersects the first bisector.

***o*-CRESOL**

Analytical-reagent grade *o*-cresol (purity > 99%), was used as the adsorbate. A stock solution was prepared by dissolving required amount of *o*-Cresol in double distilled water. Different initial concentrations (C_0) of *o*-cresol, in the range of 25-100 mg/L, were obtained by successive dilutions. *o*-Cresol concentration was determined by UV absorption at 270 nm wave-length using a calibrated UV-Visible Perkin Elmer spectrophotometer.

ADSORPTION EXPERIMENTAL PROCEDURE

Adsorption process was performed as a function of contact time, pH, initial concentrations of the *o*-cresol and temperature using an AC adsorbent amount of 1g and adsorbate volume of 100 mL (0.1 L) of *o*-cresol determined concentrations (cited in the previous paragraph). The contact time between solid–liquid were from 0 to 120 min; pH was varied from 2 to 12 and the temperature from 20 to 80 °C. The removal yield (%) and the of equilibrium adsorption q_e (mg/g) were calculated from the following Equations 1 and 2, respectively:

$$\text{Yield (\%)} = \frac{(C_i - C_{eq})}{C_i} \times 100 \quad [1]$$

$$q_e \text{ (mg/g)} = \frac{X}{m} = \frac{(C_i - C_{eq})}{m} \times V \quad [2]$$

where C_i is the initial concentration (mol/L) and C_{eq} is the equilibrium concentration (mol/L). V is the volume of the solution (L), m is the mass of adsorbent (g) and X is mass of *o*-cresol adsorbed (mg).

KINETICS STUDY

In order to understand the mechanism and dynamism of adsorption, five kinetic models have been chosen pseudo, first-order (Equation 3), pseudo second-order (Equation 4) and Elovich (Equation 5) (19). In addition, intra-particle diffusion (Equation 6) (20) and external diffusion (Equation 7) (21) were studied, too:

$$\ln(q_e - q_t) = \ln q_e - K_1 \cdot t \quad [3]$$

$$\frac{t}{(q_e - q_t)} = \frac{t}{q_e} + K_2 \cdot t \quad [4]$$

where, K_1 (min^{-1}) is pseudo-first-order kinetic constant, and K_2 represents pseudo-second-order kinetic constant.



$$q_t = \frac{\ln(\alpha_E \times \beta_E)}{\beta_E} + \frac{1}{\beta_E} \cdot \ln t \quad [5]$$

where β_E (g/mg) parameter related to the extent of surface coverage and activation energy, and α_E (mg/g.min) represents initial adsorption rate.

$$q_t = K_i t^{\frac{1}{2}} \quad [6]$$

where q_t is amount of adsorbate on the surface of the adsorbent at time t , mg/g; K_i is the intra-particle rate constant, mg/(g·min^{1/2}).

$$\ln \left(\frac{C_\sigma - C_e}{C_r - C_e} \right) = k \left(\frac{a}{V} \right) t = k' t \quad [7]$$

k' is the external rate constant (min⁻¹) and a is the solid/liquid interface area.

ISOTHERM STUDY

Adsorption isotherms have an important role in the determination of adsorbent capacity. The obtained results of the influence of the initial *o*-cresol concentration on AC adsorption during this study were used to draw them. There are many theoretical models that have been developed to describe adsorption isotherms. However, the models of Freundlich (Equation 8) and also of Langmuir (Equation 9), Elovich (Equation 10) and Temkin (Equation 11) (19), Dubinin Radushkevich (Equation 12) (22), Kiselev (Equation 13) (23) and Fowler Guggenheim (Equation 14) (24) allowed to deduce the main parameters characterizing each model as shown below:

$$\log (q_e) = \log (K_F) + n \log (C_e) \quad [8]$$

where K_F (mg/L) and n are Freundlich constants related to the adsorption capacity and adsorption intensity, respectively.

$$\frac{1}{q_e} = \frac{1}{C_e} \frac{1}{q_m K_L} + \frac{1}{q_m} \quad [9]$$

K_L (L/mg) is Langmuir constant and q_m theoretical maximum adsorption capacity (mg/g).

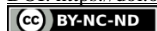
$$\ln \frac{q_e}{C_e} = \ln (q_m K_E) - \frac{q_e}{q_m} \quad [10]$$

K_E (L/mg) is the Elovich constant.

$$q_e = B_T \ln K_T + B_T \ln C_e \quad [11]$$

where K_T (L/mg) is Temkin constant, T (K) is temperature and B_T (J/mol) is related to the activation energy.

$$\ln (q_e) = \ln (q_{mDR}) - K_D \varepsilon^2 \quad [12]$$



where K_D is is Dubinin-Radushkevich constant, ε (kJ.kmol⁻¹) is potential of Polanyi = $RT \ln(1 + \frac{I}{C_e})$; R is the universal gas constant (8.314 J/mol.K) and E is mean adsorption energy $E = \frac{1}{\sqrt{K_D}}$.

$$\frac{I}{C_e(1-\theta)} = \frac{K_i}{\theta} + K_n K_n \quad [13]$$

where K_i is Kiselev equilibrium constant (L/mg) and K_n is equilibrium constant of the formation of complex between adsorbed molecules, θ the fractional coverage.

$$\ln\left(\frac{C_e(1-\theta)}{\theta}\right) = -\ln K_{FG} + \frac{2W\theta}{RT} \quad [14]$$

where K_{FG} is the Fowler–Guggenheim equilibrium constant (L/mg) and W (kJ mol⁻¹) is the interaction energy between adsorbed molecules.

THERMODYNAMIC STUDY

Thermodynamic properties such as standard enthalpy (ΔH_{ads}), entropy (ΔS_{ads}) and Gibbs free energy (ΔG_{ads}) are essential for the study of any adsorption system. These properties determine the nature of adsorption and spontaneity. These thermodynamic parameters of adsorption were carried out at four different temperatures: 25, 45, 60, 80 °C and were calculated using the following equations (19, 24):

$$\ln K_p = \frac{\Delta S_{ads}}{R} - \frac{\Delta H_{ads}}{RT} \quad [15]$$

$$\Delta G = \Delta H_{ads} - T \Delta S_{ads} \quad [16]$$

The apparent equilibrium constant (K_d) of adsorption is defined as:

$$K_d = \frac{C_{ads}}{C_{eq}} \quad [17]$$

where, K_p is the thermodynamic equilibrium constant and it is the ratio of concentration of adsorbate in the solid and liquid phases. ΔH_{ads} and ΔS_{ads} were derived from the slope and intercept of the linear plot (i.e., Van't Hoff plot) of $\ln K_p$ versus $1/T$, respectively.

RESULTS AND DISCUSSION

CHARACTERIZATION OF ADSORBENT

The adsorption/desorption curve of the AC prepared from olive pomace (Figure 1a) shows a hysteresis for which desorption branch joins the adsorption branch for a relative pressure equal to 0.42 at 77 K. This hysteresis is significant of the presence of constituent mesopores of a stable structure (type IV isotherm) (25). In addition, the obtained results show that the AC has a surface area equal to 651 m²/g, a pore volume of 0.280385 cm³/g.



A large specific surface area permits high adsorption. The pH_{pzc} is an important parameter based on the determination of the range of pH sensibility and allows the active surface and adsorption capacities to be predicted (26). The pH_{pzc} value of AC found was equal to 3.01 (Figure 1b).

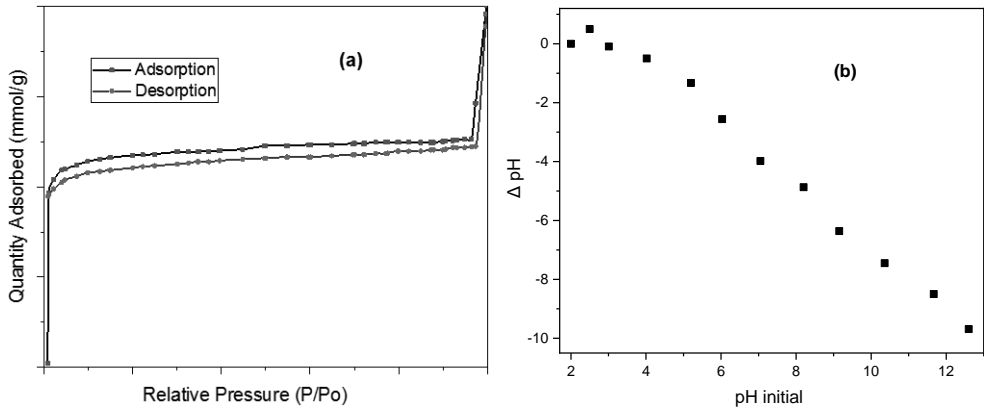


Figure 1. N₂ adsorption-desorption isotherm of AC (a) and the pH point of zero charge (pH_{pzc}) (b)

ADSORPTION STUDIES

Effect of adsorbent amount

To investigate the effect of the adsorbent dose on the efficiency of the adsorption process, a series of experiments were conducted with various adsorbent amounts of AC from 0.25 to 3 g in 100 mL of 50 mg/L *o*-cresol solution.

The effect of adsorption amount on adsorption is shown in Figure 2.

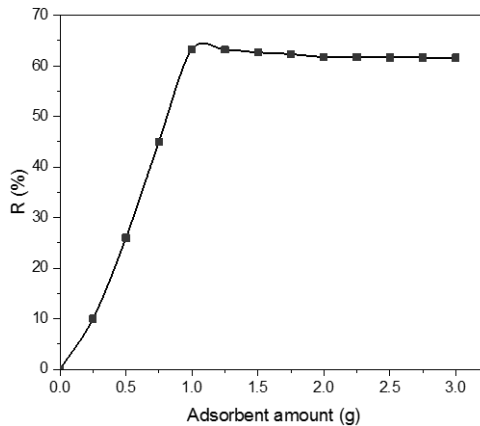


Figure 2. Effect of adsorbent amount on *o*-cresol adsorption (pH = 6.8, Time = 120 min, T = 25 °C and C_i = 50 mg/L)



As the mass of the adsorbent increased, the adsorption yields also increased to 63.25%. This is due to the presence of more active sites on the surface (27). The maximum adsorption efficiency of *o*-cresol was achieved with 1 g of AC. In addition, it is clear that an increase in the adsorbent mass above 1 g saturates the surface of the AC adsorbent and stops the adsorption phenomenon. In this case, it can be said that the adsorption equilibrium of *o*-cresol on AC is reached.

Effect of initial pH on the adsorption

The pH of the solution is one of the most important parameters affecting adsorption processes because it affects the surface charge of the adsorbent, the degree of ionization and speciation of the pollutants (28). The effect of initial pH on adsorption of *o*-cresol was studied with 50 mg/L initial concentration and 1 g optimum AC amount.

Figure 3 shows the influence of solution pH on *o*-cresol removal by AC in the pH range of 2 to 12. The *o*-cresol adsorption decreases with the increase of pH. The maximum *o*-cresol removal obtained at pH lower than pH_{pzc} ($pH_{pzc}=3.01$) can be explained by the fact that at this pH range the AC surface is charged positively and *o*-cresol was protonated (29). This creates a strong electrostatic interaction between *o*-cresol molecule carbon surface. However, with the increase of pH solution up to pH_{pzc} , *o*-cresol becomes more dissociated and AC surface is charged negatively leading to increased electrostatic repulsion force between the anionic *o*-cresol form and OH^- groups on AC surface and between phenolate-phenolate anions in solution (30) resulting in a decrease of *o*-cresol adsorption yields. Taking into account the obtained results, the rest of experiments were carried out at pH 2.6.

Effect of contact time and initial concentration

The effect of *o*-cresol initial concentration on the adsorption yield is reported in Figure 4. When initial *o*-cresol concentration increased from 25 to 100 mg/L, the adsorption yields on AC increased from 19.33 to 75.15%. The time evolution of the amount adsorbed *o*-cresol indicates that the equilibrium time was reached at about 60 min for all the initial concentrations. Two kinetics regions were observed: the first one is characterized by a high adsorption rate due to the high initial number of free sites in activated carbon available and the driving force for the mass transfer is greater. Therefore, *o*-cresol reaches easily the adsorption sites of AC. As time progresses, the number of free sites in AC decreases and the non-adsorbate molecules are assembled at the surface thus limiting the capacity of adsorption. The increase of loading capacities of AC with increasing *o*-cresol concentration is may be due to the higher π - π interaction between *o*-cresol and the surface function of activated carbon. The π - π interaction is usually the mean involved mechanism of *o*-cresol adsorption (31, 32).

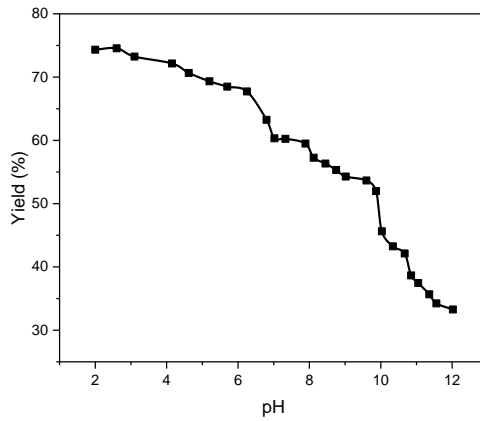


Figure 3. Effect of pH on *o*-cresol adsorption ($m = 1$ g, Time = 120 min, $T = 25$ °C and $C_i = 50$ mg/L)

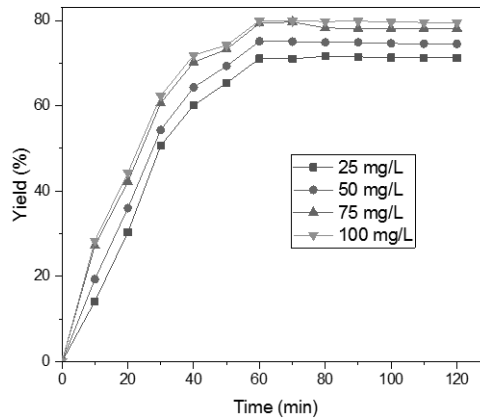


Figure 4. Effect of initial concentration *o*-CRESOL adsorption

Effect of the temperature

The temperature effect on adsorption of *o*-cresol on AC was examined at a range from 20 °C to 80 °C and shown in Figure 5. The yield of adsorbed *o*-cresol increased until it reaches the maximum adsorption of 83.66% at 30 °C. Then, yield of *o*-cresol adsorption decreased gradually with the increase in temperature. This can be attributed to the possible damage of adsorption sites at elevated temperatures.

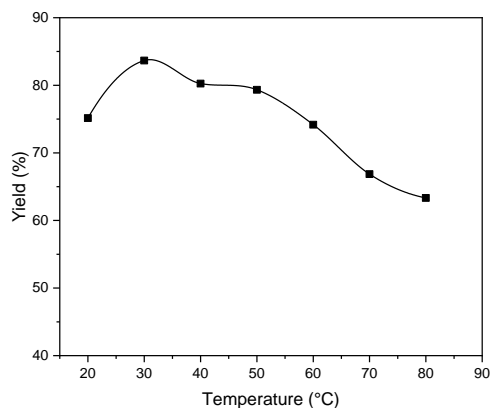
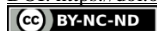


Figure 5. Effect of the temperature on the *o*-cresol adsorption

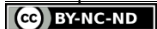
KINETIC STUDY

Adsorption *o*-cresol kinetics on AC was studied by fitting experimental data. The obtained parameters, the experimental adsorbed quantity (q_e) and correlation coefficients were calculated from the equations cited previously (See section 2.4) and regrouped in Table 1.

Table 1. Parameters and correlation coefficients of adsorption kinetic models applied to experimental data of *o*-Cresol adsorption on AC

Kinetic models	Constants	Results
Pseudo first-order	K_1 (min^{-1})	0.045
	q_e ($\text{mg}\cdot\text{g}^{-1}$)	3.420
	R^2	0.830
Pseudo second-order	K_2 (min^{-1})	0.028
	q_e ($\text{mg}\cdot\text{g}^{-1}$)	4.040
	R^2	0.995
Elovich	α_E ($\text{mg}\cdot\text{g}^{-1}\cdot\text{min}$)	3.460
	β_E ($\text{g}/\text{mg}\cdot\text{min}^{-1}$)	0.614
	R^2	0.922
Intra-particle diffusion	K_i ($\text{mg}/(\text{g}\cdot\text{min}^{1/2})$)	0.366
	R^2	0.821
External diffusion	K_f (min^{-1})	0.011
	R^2	0.632

According to these values, the pseudo second order and Elovich models present very significant regression coefficient values ($R^2 > 0.90$), but the pseudo-second order model presents a correlation coefficient value the highest ($R^2 = 0.995$). It can therefore deduce that



the pseudo-second order model is the best model describes the adsorption process of *o*-cresol on the prepared activated carbon. Also, the value of the quantity adsorbed calculated by the kinetic model of pseudo-second order 4.04 mg/g is very close to the value of experimental quantity adsorbed (3.82 mg/g).

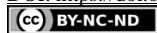
ISOTHERM STUDY

The values of the calculated constants of isotherms are shown in Table 2. From these modeling results, it can be observed that most of the linear models represent well the adsorption isotherms of *o*-cresol on the prepared AC with non-negligible correlation coefficients. The values of the regression coefficients indicate that the adsorption process of *o*-cresol is described in a favorable way by the Freundlich isotherm with excellent linear regression coefficients ($R^2 = 0.996$) which is very close to unity.

Table 2. Parameters and correlation coefficients of isotherms models applied to experimental data of *o*-Cresol adsorption on AC

Isotherm models	Constants	Results
Freundlich	K_F (mg.g ⁻¹) (L.mg ⁻¹)	0.090
	n	1.510
	R^2	0.996
Langmuir	K_L (L.mg ⁻¹)	0.023
	q_m (mg.g ⁻¹)	8.400
	R^2	0.974
Elovich	q_m (mg.g ⁻¹)	12.500
	k_E (L.mg ⁻¹)	0.017
	R^2	0.929
Temkin	B_T (Kj.mol ⁻¹)	-10.490
	K_T (L.mol ⁻¹)	0.174
	R^2	0.943
Dubinin Radushkevich	K_D (mol.j ²)	6.10^{-5}
	R^2	0.796
Kiselev	K_i (L.mg ⁻¹)	-0.022
	K_n (L.mg ⁻¹)	-10.810
	R^2	0.500
Fowler Guggenheim	K_{FG} (L.mg ⁻¹)	0.020
	W (Kj.mol ⁻¹)	-3702
	R^2	0.990

In addition, the value of n (Freundlich constant) is greater than 1, it means that the adsorption is favorable (the intensity of the adsorption is high) with the formation of strong bonds between the adsorbate and the adsorbent in the studied temperature range. The adsorption is an endothermic process; it can be explained by the increase of the temperature



with the value of K_F (33). Indeed, the value of the regression coefficient shows that the Fowler Guggenheim model ($R^2=0.99$) is adequate for a good description of this adsorption of *o*-Cresol on the prepared AC. The regression coefficients were not satisfactory for the isotherm of Elovich, Kiselev and Dubinin Radushkevich, so they do not model the isotherm of adsorption of *o*-Cresol on activated carbon.

THERMODYNAMIC STUDY

The thermodynamic parameters: free energy (ΔG_{ads}), enthalpy (ΔH_{ads}) and entropy (ΔS_{ads}) are regrouped in Table 3. The enthalpy (ΔH_{ads}) is positive, which implies that the adsorption process is endothermic. It is also noticed that ΔG_{ads} increases with the increase in the temperature of the solution. The result can be explained by the fact that adsorption becomes very difficult and disadvantaged when the temperature becomes very high (33). Positive values of ΔG_{ads} and its increase with temperature indicate an increase in disorder during adsorption, the randomness increases at the solid-solution interface during this fixation process. This can be explained by the redistribution of energy between the adsorbent and the adsorbate. The *o*-cresol adsorption process is a physical adsorption type when the ΔG_{ads} values are less than 40 KJ/mol. The negative value of ΔS_{ads} shows that the adsorption takes place with an increase in the order at the solid-solution interface.

Table 3. Thermodynamic parameters of *o*-Cresol adsorption on AC

Parameters	T (K)	ΔG_{ads} (KJ/mol)	ΔH_{ads} (KJ/mol)	ΔS_{ads} (J/mol)
Results	293	2.204	16.279	-60.240
	301	1.675		
	312	2.489		
	333	3.763		
	333	3.874		
	345	4.587		
	357	5.192		

CONCLUSION

In this study, the removal of *o*-cresol from aqueous solution by adsorption on olive pomace activated carbon (AC) was developed. This is in order to protect the environment by using the waste from olive oils production (olive pomace) in the elimination of another type of industrial waste (*o*-cresol, a toxic phenolic derivative). The characterization of the activated carbon prepared with chemical activation from olive pomace showed a specific surface area equal to 651 m²/g with the presence of mesopores.

The obtained results show that the equilibrium of sorption is reached within 60 min with a removal yield of 83.66%. Indeed, the experimental adsorbed quantity of adsorbent is 3.82 mg/g with *o*-cresol concentration of 50 mg/L, T = 30 °C and pH 2.6 for a good adsorption. Some kinetics, isotherms and thermodynamics adsorption studies were investigated: The kinetics of *o*-cresol adsorption on AC follows the pseudo-second order model and fitted the



Freundlich model. The results demonstrated that the adsorption is a physical and endothermic process.

In the end, prepared AC from olive pomace is a promising material for *o*-cresol elimination and may also be effective in removing other pollutants.

Acknowledgements

The Algerian Directorate General of Scientific Research and Technological Development (DGRSDT), and the Algerian Ministry of Higher Education and Scientific Research (MESRS) are greatly thanked.

REFERENCES

1. Li, M.; Liu, Y.; Yang, G.; Sun, L.; Song, X.; Chen, Q.; Bao, Y.; Luo T.; Wang, J. Microstructure, physicochemical properties, and adsorption capacity of deoiled red raspberry pomace and its total dietary fiber, *LWT*, **2022**, *153*, 112478. Doi: 10.1016/j.lwt.2021.112478
2. Gao, C.; Zhao, S.; Yagiz, Y.; Gu, L. Static, Kinetic, and Isotherm Adsorption Performances of Macroporous Adsorbent Resins for Recovery and Enrichment of Bioactive Procyanidins from Cranberry Pomace. *Journal of food Sci.* **2018**, *83*(5), 1249-1257. Doi: 10.1111/1750-3841.14142
3. Chand, P.; Pakade, Y.B. Synthesis and characterization of hydroxyapatite nanoparticles impregnated on apple pomace to enhanced adsorption of Pb (II), Cd (II), and Ni (II) ions from aqueous solution. *Environ. Sci. Pollut Res.* **2015**, *22*(14), 10919-10929. Doi: 10.1007/s11356-015-4276-2
4. Wu, L.; Melton, L.D.; Sanguansri L.; Augustin, M. A. The batch adsorption of the epigallocatechin gallate onto apple pomace. *Food chemistry.* **2014**, *160*, 260-265. Doi: 10.1016/j.foodchem.2014.03.098
5. Wu, L.Y. ; Guo, Y.L.; Cao, L.L.; Jin, S.; Lin, H.Z.; Wu, M.Y.; Lin J.K.; Ye, J.H. Application of NaOH-HCl-Modified Apple Pomace to Binding Epigallocatechin Gallate. *Food Bioprocess Technol.* **2016**, *9*, 917-923. Doi: 10.1007/s11947-016-1683-4
6. Singh, R.J.; Martin, C.E.; Barr D.; Rosengren, R.J. Immobilised apple peel bead biosorbent for the simultaneous removal of heavy metals from cocktail solution. *Cogent Environ Sci.* **2019**, *5*, 1673116. Doi: 10.1080/23311843.2019.1673116
7. Perra, M.; Bacchetta, G.; Muntoni, A.; De Gioannis, G.; Castangia, I.; Rajha, H.N.; Manca, M. L.; Manconi, M. J. An outlook on modern and sustainable approaches to the management of grape pomace by integrating green processes, biotechnologies and advanced biomedical approaches. *Funct. Foods.* **2022**, *98*, 105276. Doi: 10.1016/j.jff.2022.105276
8. Sbai, G.; Loukli, M. Traitement Electrochimique Des Margines Et Identification Des Composés Avant Et Apres Traitement Par Chromatographie En Phase Gazeuse Couplee Par Spectroscopie De Masse. *Larhyss Journal.* **2015**, *22*, 139-152.
9. Bekri, I.; Taleb, Z.; Taleb, S.; Tlemsani, S.; Hodaifa, G.; Abdelkader, B. High adsorption capacity of thermally treated solid olive wastes to treat olive mill wastewater. *Environ Qual Manage.* **2022**, *31*(4), 391-402. Doi: 10.1002/tqem.21823
10. Marrakchi, F.; Bouaziz, M.; Hameedc, B.H. Adsorption of acid blue 29 and methylene blue on mesoporous K₂CO₃-activated olive pomace boiler ash. *Colloids and Surfaces A.* **2017**, *535*, 157-165. <http://dx.doi.org/10.1016/j.colsurfa.2017.09.014>
11. Alburquerque, J.A.; González, J.; García, D.; Cegarra, J. Agrochemical characterisation of alperujo, a solid by-product of the two-phase centrifugation method for olive oil extraction. *Biore-sour. Technol.* **2004**, *91*, 195-200.
12. Nieto, L.M.; Alami, S.B.D.; Hodaifa, G.; Faur, C.; Rodriguez, S.; Gimenez, J.A.; Ochando, J. Adsorption of iron on crude olive stones. *Ind Crops Prod.* **2010**, *32*(3), 467-471.



13. Bohli, T.; Ouederni, A.; Fiol, N.; Villaescusa, I. Evaluation of an activated carbon from olive stones used as an adsorbent for heavy metal removal from aqueous phases. *C. R. Chimie.* **2015**, *18*(1), 88-99. <http://dx.doi.org/10.1016/j.crci.2014.05.009>
14. Kandah, M.I.; Meunier, J.-L. Removal of Nickel Ions from Water by Multi-Walled Carbon Nanotubes. *Journal of Hazardous Materials.* **2007**, *146*, 283-288.
15. Taleb, Z.; Ramdani, A.; Berenguer, R.; Ramdani, N.; Adjir, M.; Taleb, S.; Morallón, E.; Nemnich S.; Tilmatine, A. Combined ozonation process and adsorption onto bentonite natural adsorbent for the o-cresol elimination. *Int. J. Environ. Anal. Chem.* **2021**, *103*(5), 977-994. Doi: 10.1080/03067319.2020.1865335
16. Gracioso, L. H.; Vieira, P. B.; Baltazar, M. P. G.; Avanzi, I. R.; Karolski, B.; Nascimento, C. A. O.; Perpetuo, E. A. Removal of phenolic compounds from raw industrial wastewater by *Achromobacter* sp. isolated from a hydrocarboncontaminated area. *Wat. and Environ. J.* **2019**, *33*(1), 40-50. Doi: 10.1111/wej.12367
17. Gharib, H.; Ouederni, A. Transformation du grignon d'olive Tunisien en charbon actif par voie chimique à l'acide phosphorique- Processing olive pomace Tunisian activated carbon chemically with phosphoric acid. Recent Advances in Process Engineering, SFGP, Paris, France, 2005, 92.
18. Altenor, S.; Carene, B.; Emmanuel, E.; Lambert, J.; Ehrhardt, J. J. and Gaspard, S. Adsorption studies of methylene blue and phenol onto vetiver roots activated carbon prepared by chemical activation. *J. Hazard. Mater.* **2009**, *165*, 1029. Doi: 10.1016/j.jhazmat.2008.10.133
19. Tlemsani, S.; Taleb, Z.; Piraült-Roy L. and Taleb, S. Temperature and pH influence on Diuron Adsorption by Algerian Mont-Na Clay. *Int. J. Environ. Anal. Chem.* **2022**. Doi: 10.1080/03067319.2022.2060093
20. Soenmezay, A.; Öncel, M.S.; Bektaş, N. Adsorption of lead and cadmium ions from aqueous solutions using manganoxide minerals, *Trans. Nonferrous Met. Soc. China.* **2012**, *22*(12), 3131-3139. Doi: 10.1016/S1003-6326(12)61765-8
21. Belaid, K.; Kacha, S. Study of the kinetics and thermodynamics of the adsorption of a basic dye on sawdust. *J. Wat Sci.* **2011**, *24*(2), 131-144.
22. Ayawei, N.; Ebelegi, A.N.; Wankasi, D. Modelling and Interpretation of Adsorption Isotherms. *J. chem.*, **2017**. 3039817. Doi: 10.1155/2017/3039817
23. Hamdaoui O.; Naffrechoux, E. Modeling of adsorption isotherms of phenol and chlorophenols onto granular activated carbon Part I. Two-parameter models and equations allowing determination of thermodynamic parameters *J. Hazard. Mater.* **2007**, *147*, 381-394. Doi: 10.1016/j.jhazmat.2007.01.021
24. Lu, M.; Zhang, Y. M.; Guan, X. H.; Xu, X. H.; Gao, T. T. Thermodynamics and kinetics of adsorption for heavy metal ions from aqueous solutions onto surface amino-bacterial cellulose. *Trans. Nonferrous Met. Soc. China.* **2014**, *24*, 1912-1917. Doi: 10.1016/S1003-6326(14)63271-4
25. Thommes, M.; Kaneko, K.; Neimark, A.V.; Olivier, J.P.; Rodriguez-Reinoso, F.; Rouquerol, J.; Sing, K.S. Physisorption of gases, with special reference to the evaluation of surface area and pore size distribution (IUPAC Technical Report). *Pure Appl. Chem.* **2015**, *87*(9-10), 1051-1069. Doi: 10.1515/pac-2014-1117
26. Pintor, M.J.; Jean-Marius, C.; Jeanne-Rose, V.; Taberna, P.L.; Simon, P.; Gamby, J.; Gadiou, R.; Gaspard, S. Preparation of activated carbon from Turbinaria turbinata seaweeds and its use as supercapacitor electrode materials. *C. R. Chimie.* **2013**, *16*, 73-79.
27. Boudia, R.; Mimanne, G.; Benhabib, K.; Pirault-Roy, L. Preparation of mesoporous activated carbon from date stones for the adsorption of bemacid red. *Water Sci. Technol.* **2019**, *79*(7), 1357-1366. Doi: 10.2166/wst.2019.135 28.
28. Maleki, A.; Mahvi, A.H.; Ebrahimi, R.; Khan, J. Evolution of Barley straw and its Ash in Removal of Phenol from Aqueous System. *Word Appl. Sci. J.* **2010**, *8*(3), 369-373.
29. Lü, G.; Hao, J.; Liu, L.; Ma, H.; Fang, Q.; Wu, L.; Wei, M.; Zhang, Y. The Adsorption of Phenol by Lignite Activated Carbon. *Chin. J. Chem. Eng.* **2011**, *19*(3), 380-385.



30. Mareno-Castilla, C. Adsorption of organic molecules from aqueous solutions on carbon materials. *Carbon*. **2004**, *42*, 83-94.
31. Li, D.; Wu, Y.; Feng, L.; Zhang, L. Surface properties of SAC and its adsorption mechanisms for phenol and nitrobenzene. *Bioresour. Technol.* **2012**, *113*, 121-126. Doi: 10.1016/j.biortech.2012.02.130
32. Li, Y.; Du, Q.; Liu, T.; Peng, X.; Wang, J.; Sun, J.; Wang, Y.; Wu, S.; Wang, Z.; Xia Y.; Xia, L. Comparative study of methylene blue dye adsorption onto activated carbon, graphene oxide, and carbon nanotubes. *Chem. Eng. Res. Des.* **2013**, *91*(2), 361-368. Doi: doi.org/10.1016/j.cherd.2012.07.007
33. He, J. Hong, S. Zhang, L. Gan F.; Ho, Y.S. Equilibrium and thermodynamic parameters of adsorption of methylene blue onto rectorite. *Fresenius Environ. Bull.* **2010**, *19*(11), 2651-2656.